Chapter 7

Synthesis of Titanium Dioxide Nanorod Arrays Using a Facile Aqueous Sol-Gel Route for Ultraviolet Photosensor Applications

Marmeezee Mohd. Yusoff,
Mohamad Hafiz Mamat and
Mohamad Rusop Mahmood

Additional information is available at the end of the chapter

http://dx.doi.org/10.5772/intechopen.68460

Abstract

In this chapter, we review the state of the art of aqueous sol-gel route for ultraviolet (UV) photosensor applications based on the nanostructured TiO_2. The performance of UV photosensor is associated with the high surface-to-volume ratio, porosity, surface defects, light trapping, and the intensity of the UV radiation. One-dimensional (1D) growth of TiO_2 nanorod arrays (TNAs) offers an enhance charge carrier mobility to overcome the photocurrent loss due to the existence of multiple grain boundaries in granular-like and porous nanostructures. Photoelectrochemical cell (PEC)-based device structure is preferred in TNA-based UV photosensor due to its low cost, facile fabrication process, high contact area, low recombination of the excitonic charge carriers, high photocurrent gain, and fast response and recovery times. It also could work in applied bias mode, as well as in "self-powered" mode. Our study has introduced a new one-step method to deposit a thin film TNA on an FTO-coated glass substrate at low temperature and a rapid process using a facile glass container. The fabricated PEC-based UV photosensor using the deposited TNAs has successfully shown its potential in the application of UV photosensor.

Keywords: TiO_2, nanorod arrays, UV photosensor

1. Introduction

Titanium dioxide (TiO_2) nanostructures emerged as one of promising materials for electronic device applications such as diodes, transistors, memristors, sensors, and solar cells. TiO_2 with numerous nanostructures yield a unique, expedient, and novel size and shape-dependent

characteristics that are significant for high performance devices. TiO_2 nanorod array (TNA) is one of the favorable nanostructures that become tremendously significant in optoelectronic applications due to its large surface area, high electron mobility, and efficient light scattering ability. The physical tunings of its active surface area by controlling the diameter size and length of the nanorod, for instance, improve its functionality and sensitivity, thus enhancing the performance of the device. In ultraviolet (UV) photosensor application, these great characteristics of the TNAs enable the fabrication of a device with high responsivity and reliability. Although there are many methods available to synthesis the TNAs, aqueous sol-gel-based method compromise numerous advantages including a facile low temperature and low-time deposition, uniform and large-scale deposition-compatible, and producing excellent TNA crystalline properties. In this chapter, synthesis of TNAs via aqueous sol-gel methods will be discussed for the application of UV photosensor. The structural, optical, and electrical properties of deposited TNAs will be investigated. The performance of the fabricated TNA-based UV photosensor will also be discussed.

2. Ultraviolet photosensor using TiO_2 nanomaterials

Recent developments in the field of semiconductor have led to a renewed interest in TiO_2 nanostructures due to their unique and excellent properties in optic, electronic, and photonic devices. TiO_2 is basically a nontoxic material, physically stable and chemically robust to the environments that has extensive applications, for instance in photocatalytic activities, detecting devices, biomedical devices, and solar cell. In general, TiO_2 is an n-type semiconductor in natural, intrinsically prone to UV radiation and distinguish from visible light region due to its wide band gap energy of around 3.2 eV at an ambient temperature [1, 2]. Thus, TiO_2 has an excellent UV absorption, particularly in thin film based on its optical property. The downsize of TiO_2 particle in the nanoscale region also received excessive attention due to its distinct characteristics exhibited in electrical, mechanical, chemical, and others due to its quantum confinement effects, compared to their bulk component. Significant part of nanostructured TiO_2 material is due to high surface-to-volume ratio and high porosity, which increases the reactive surface area in particular reaction cycles in definite volume to achieve the requirement of high performance and high efficiency device applications. In addition to high surface-to-volume ratio, the number of atoms on the surface area plays the most important role of the overall number of atoms in the nanostructured materials, which enhance the thermal stability due to low surface energy generated compared to their bulk. This property is considered unique for certain electronics applications [3].

UV photosensor for detecting UV radiation is of interest and an important aspect in modern industries and environmental monitoring. In medical sector, it could be used to monitor the UV radiation treatment on patient with diseases such as rickets, psoriasis, eczema and jaundice, as well as slimming treatment in beauty and health sector, from having a prolonged exposure which may be attributed to chronic and acute health side effects. The fundamental of UV photosensor is basically explained by the generation of photocurrent from the exposure of incident UV radiation on few semiconductor materials with wide energy band gap. This

http://dx.doi.org/10.5772/intechopen.68460

phenomenon comprises a number of mechanisms, including the light absorption, photogeneration of charge carriers, and charge carriers transport [4]. The concepts of conductivity in this phenomenon are central to the amount of photogenerated charge carriers (electrons and holes) per absorbed photon or quantum yield and the transportation of generated charge carriers. Overall, the gain of the photogenerated current under the exposure of UV radiation typically comprises of few elements such as lifetime of the charge carriers, light trapping, charge carriers trapping and mobility, and the defects on the surface of the materials. In addition, the nanostructure and electrical properties of the materials such as conductivity and resistivity also play a major role in optimizing the performance of the UV photosensor.

Extensive research has been performed regarding UV photosensor based on TiO_2 nanostructures as the detecting components. Okuya et al. developed TiO_2 thin film-based UV sensors using a spray pyrolysis deposition (SPD) technique [5]. TiO_2 film was prepared using the sol-gel consisted of 0.05 M of titanium (IV) oxy acetylacetonate, ethanol solution, and aluminum (III) acetylacetonate as an additive. They produced TiO_2 thin films at 200 nm in $CuO/TiO_2/SnO_2$ p-i-n junction on a glass substrate and revealed that the used solvent with upper boiling limit has benefited for a particle growth due to wettability to a substrate and thus produced higher porosity. High porosity exhibited the maximum intensity due to improvement of light absorption from light scattering by small particles within the porous nanostructures. The doping of aluminum to TiO_2 layer, to some extent, was also attributed to increase the intensity by the reduction of carrier density, which enhanced the light absorption in correlation with low scattering of photogenerated carriers. The maximum intensity achieved was 12.5×10^{-4} A/W from 2 at % aluminum-doped TiO_2 films under the light intensity of 50 $\mu W/cm^2$ at the wavelength of 345 nm.

A UV photosensor based on metal-semiconductor-metal (MSM) structure using nanocrystalline TiO_2 thin films with Au Schottky contact was demonstrated through a sol-gel spin-coating technique [6]. An Au film was deposited by radio frequency (RF) magnetron sputtering to construct interdigitated $Au/TiO_2/Au$ structure with 260 nm thickness of Au film. Their study reported that the highest photoresponsivity at 199 A/W under 260 nm irradiation at 5 V bias, with the dark current at 1.9 nA. They also suggested that the high responsivity was primarily due to the reduction of Schottky barrier introduced by surface defects, which attributed to more carriers getting across the barrier and subsequently increased the measured photogenerated current. Moreover, the existence of neutral photoconductor region from the wide gap between the Au electrodes introduced high gain was also responsible for the high photoresponsivity of fabricated device. At the same time, the slow photoresponse, which occurred in MSM structure mostly, was primarily due to the defect in the nonocrystalline neutral region and could be further improved by enhancements on material and structure.

Han et al. introduced a UV photosensor based on a p-n junction consisting of n-type TiO_2 nanocrystals and p-type poly(9,9-dihexylfluorene) (PFH) [7]. The sol-gel consisted of oleic acid, triethylamin, NH_4HCO_3, cyclohexane, and $Ti(OBu)_4$ was mixed together at room temperature for the synthesization of TiO_2 nanocrystals via solvothermal method at 180°C for 20 hours. The synthesized TiO_2 nanocrystals were then mixed with the PFH solution to form a hybrid dispersion, before spin coated on the substrate. The sensitivity of the fabricated device

was 2.94 mA/W under UV irradiation and 6.92 mA/W under 365 nm UV light. The work suggested that TiO_2 content was in correlation with the photogenerated current density, which is related to the deviation of the size of the interface between the two components that attributed to the agglomeration of TiO_2 nanoparticles. It was also mentioned that the high crystallinity of TiO_2 nanocrystals and a small size distribution were very significant for chemicophysical property, which enhanced the electron-transporting mechanism in the fabricated device.

One study by Vigil et al. examined the trend in a sealed two-electrode photoelectrochemical cell (PEC) using a double-layer of nanocrystalline TiO_2 [8]. A double layer of TiO_2 (**Figure 1**) was introduced through a "doctor-blading" technique for a mesoporous TiO_2 (~5 μm thickness) layer on top, while the bottom TiO_2 film (~100 nm thickness) obtained via microwave-assisted chemical bath deposition (MW-CBD) on transparent conducting oxide (TCO)-coated glass as contact electrodes. The sol-gel was consisted of the aqueous solutions of $(NH_4)_2TiF_6$ solution and H_3BO_3. The fabricated device showed an *I–V* curve of a junction diode characteristic. The measured short circuit photogenerated current values was 0.3–0.4 mA under UV radiation (λ = 340 nm) and linearly dependent on radiation intensity. The chapter suggested that the mesoporous structure with nanocrystallites (20–30 nm in size) allowed the penetration of electrolyte, which rapidly captured the holes through the iodide ions in the electrolyte from the high surface area of TiO_2 during the irradiation and thus hindered the recombination of electron-hole pairs for longer diffusion of electrons to TCO anode contact. They also proposed that the existence of the dense thin film deposited on top of the TCO inhibited the recombination of electrons in the TCO with species in the electrolyte.

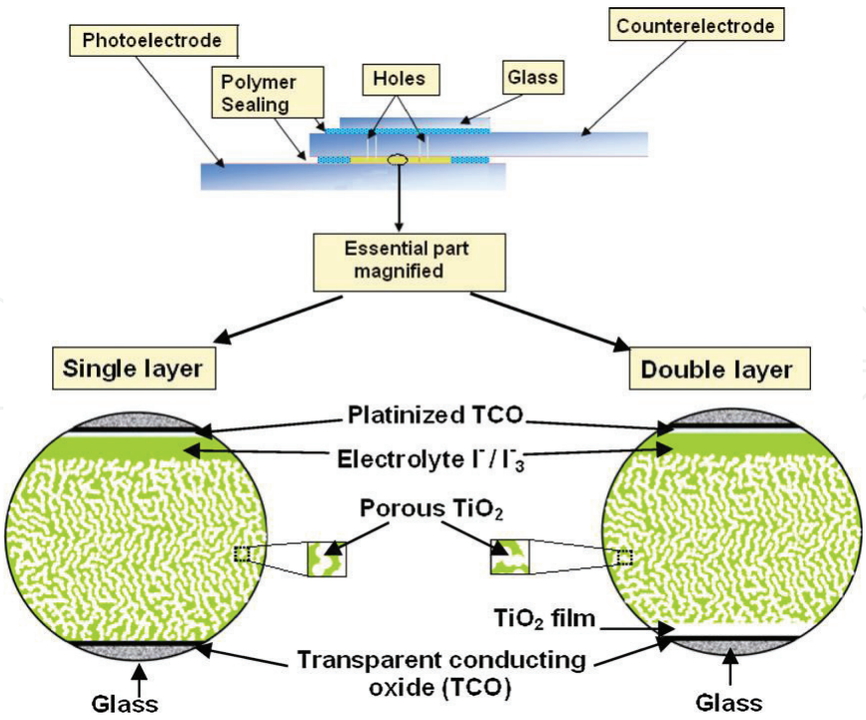

Figure 1. Schematic of UV photosensor based on photoelectrochemical cell (PEC) using a double-layer of nanocrystalline TiO_2 [8].

Another study of two-electrode PEC-based self-powered UV photosensor using a nanocrystalline TiO_2 was reported by Li et al. [9]. The performance of the fabricated self-powered photosensor was described to be isolated from the surrounding environment through the unique sandwich structure of PEC. Nanocrystalline TiO_2 was deposited through a spin-coating technique for a mesoporous structure (450 nm thickness) on an FTO-coated glass substrate as a contact electrode and followed by annealing at 500°C in air for 2 hours. The sol-gel was consisted of tetrabutyltitanate, acetic acid, ethanol, poly(vinyl pyrrolidone) (PVP), *N,N*-dimethylformamide (DMF), and tri-ethanolamine (TEOA). The measured short circuit photogenerated current values was 54 mA/cm^{-2} under UV radiation (λ = 330 nm, 150 mW/cm^{-2}) at 0 V bias and linearly dependent on radiation intensity.

Xiang et al. proposed a porous and dense nanocrystalline TiO_2 films grown on the FTO-coated glass substrate using a spin-coating technique from nanosized TiO_2 particles synthesized via hydrothermal method for vertical geometry UV photosensor [10]. Both porous and dense films were prepared at the same thickness, and the porous film was consisted of particles with an average size of 30 nm. The sol-gel was consisted of titanium isopropoxide, acetic acid, DI water, and HNO_3. Polyethylene glycol was added in the sol-gel to produce the porous film. They suggested that the response time of vertical geometry photosensor was faster than the lateral geometry photosensor for MSM-based device. The *I–V* characteristic of the porous film showed better rectifying behavior than that of the dense film. The photoresponsivity measured in photovoltage of the porous film was higher than that of the dense film under the 248-nm laser pulse irradiation due to light-scattering effects, which improved the light harvesting efficiencies in the deposited film. However, the response time of the porous film was slightly longer than that of the dense film in correlation with higher defect density in the porous film. They also suggested that the dislocation direction, which was parallel to the vertical geometry of photosensor, reduced the response time than that of the lateral geometry due to the reduction of mobility fluctuation of the charge carriers.

Another report of MSM-based TiO_2 UV photosensor on the $LaAlO_3$ substrate was introduced by Lv et al. using a sol-gel spin coating technique with Pt-interdigitated electrodes on the top of TiO_2 film [11]. The sol-gel was consisted of tetrabutyltitanate ($Ti(OC_4H_9)_4$), ethanol (C_2H_5OH), CH_3COOH, acetylacetone, and DI water. A high responsivity of 31.7 A/W was achieved under the UV radiation (260 nm, 26.5 μW/cm^2) at 5 V bias. Very low dark current was reported at 50 pA, and the ratio of the photogenerated current to dark current reached 5 orders of magnitude. The device also showed fast response and recovery at the ON and OFF states, respectively. They suggested that the low dark current achieved was due to increase of Schottky barrier height between Pt and TiO_2, which attributed to a wide depletion region. The formation of a heterojunction and depletion region at the interface of $TiO_2/LaAlO_3$, and the formation of reverse-biased junction from one of the two back-to-back Schottky junctions at Pt/TiO_2 interfaces were also attributed to the reduction of the dark current. The decrease of rise time was also due to the depletion region at the interface of $TiO_2/LaAlO_3$, where a large number of electrons from the electron-hole pairs generated and separated during the irradiation of UV were drifted toward the anode electrode. Meanwhile, the significant decrease of fall time during the OFF state was due to the rapid recombination of the balanced electrons with the holes in the depletion region at the interface of $TiO_2/LaAlO_3$.

Selman et al. developed a p-n heterojunction-based UV photosensor consisted of n-type TiO_2 on the p-type silicon substrate [12]. The work involved a deposition of TiO_2 seed layer on the p-type (1 1 1)-oriented silicon wafer via radio-frequency (RF) magnetron sputtering. Chemical bath deposition (CBD) technique was performed to grow rutile TiO_2 nanorods (NRs) with an average diameter of 30–35 nm and an average length of 85 nm on the seed layer of silicon substrate. The sol-gel was consisted of titanium (III) chloride ($TiCl_3$), urea (NH_2CONH_2), and DI water. A Pt electrode (~100 nm thickness) was deposited as a front contact on the TiO_2 NRs via RF magnetron sputtering. Their study stated that the responsivity of the device was significantly improved in correlation with bias voltage, and the responsivity achieved were 164.8, 377.0, and 538.5 A/W at 3, 5, and 7 V bias, respectively, under the UV radiation (405 nm, 0.22 mW/cm^2). High responsivity was due to high density and larger and rougher surface area of the deposited TiO_2NRs, and good formation of p-n junction in the TiO_2NRs/p-Si(1 1 1) interface. In addition, high photogenerated current achieved was due to the high crystallinity structure of the deposited rutile TiO_2, with reduced grain boundaries and defects on the structure that created electron trap to hinder the transportation of the charge carriers. Moreover, high aspect ratio also increased the photogenerated current due to oxygen desorption at the surface of TiO_2NRs.

Another interesting study that utilized the MSM-based UV photosensor with a NH_4^+ modified TiO_2 film and interdigitated Au electrodes on quartz substrates was reported by Liu et al. [13]. TiO_2 was deposited using a sol-gel spin coating technique and subsequently immersed in ammonium sulfide [$(NH_4)_2S$] solution to generate NH_4^+ modified TiO_2 films. The sol-gel consisted of tetrabutyltitanate ($Ti(OC_4H_9)_4$), ethanol (C_2H_5OH), acetic acid (CH_3COOH), acetylacetone, and DI water. A high photogenerated current of 84.93 μA and responsivity of 361.07 A/W was achieved under the UV radiation (300 nm, 61.9 μW/cm^2) at 5 V bias. Surface modification of TiO_2 film also showed the decrease of rise time to 366.9 ms and dark current to 88.8 pA than that of the TiO_2 without the surface modification. They found that the decrease in the Schottky barrier height (SBH) between TiO_2 and Au was due to the generation of dipole between NH_4^+ and exposed oxygen ions, replacing the H^+ on the deposited TiO_2 surface, which increased the performance of the device.

Yang et al. fabricated an MSM-based UV photosensor with two-dimensional (2D) TiO_2 nanosheets (TiO_2NS) deposited on 150 nm thickness of Ag IDT-electrodes on a glass substrate [14]. TiO_2NS was prepared via a sol-gel hydrothermal technique and calcined at different temperatures for 2 hours. The sol-gel was consisted of tetrabutyltitanate (TBOT), HCl, polyethylene oxide-polypropylene oxide-polyethylene oxide (PEO_{20}-PPO_{70}-PEO_{20}), ethanol (EtOH), and ethylene glycol (EG). The thickness of deposited TiO_2NS was about 1–7 nm, in correlation with 2–10 stacking layers of the monolayer (0.62 nm thickness). The measured photogenerated current of 69.4 nA was achieved under the UV radiation (3 mW/cm^2) at 1 V bias, with ultralow dark current (~2.63 pA) and fast response and recovery times. Low dark current may partly attributed from the boundaries between the nanosheets, which hindered the mobility of the charge carriers.

In previous studies on the TiO_2-based UV photosensor, the application of nanostructure materials have a lot of advantages over bulk materials, comprising high photogenerated current,

high responsivity, fast response and recovery times, low power consumption, and miniaturization of the device structure. Thus far, a number of studies have highlighted the factors that are associated with the high responsivity of nanostructured devices in correlation with a high surface-to-volume ratio, surface defects, light trapping, charge carriers trapping, and high porosity [4]. The performance of the device was also dependent on the device structure and the detection mechanism of photon through the photogenerated charge carriers. Thus far, several studies have used some instances of UV photosensor based on p-i-n photodiodes, p-n junction, Schottky barrier (SB), and MSM structure, and these types of photosensors required an external bias with potential difference to hinder the recombination of the excitonic charge carriers. Such mechanism for most conventional sensors generally required an external power supply sources from batteries, or additional supplies from the controller systems for instances, which against the concept of miniaturization of future device system and also prominently reduced the independency and mobility of the detection system. Furthermore, energy supply has becoming one of the great challenges for large-scale area applications of the sensors [15]. The techniques to synthesize and deposit the TiO_2 nanostructures on the substrate are also important to be considered in addition to produce a rapid production and low-cost device. Much of the previous research has focused on the synthesization and deposition of granular-like and porous nanocrystalline TiO_2 that contributed to the enlargement of reactive surface area of detecting component. Much of the literature has also emphasized the lifetime of photogenerated charge carriers in conjunction to reduce the recombination rate of electron-hole pairs. The charge carrier's transportation is also relatively important in maximizing the overall photocurrent gain, as the effective charge carrier mobility is desired for high efficiency devices.

3. TiO_2 nanorod arrays (TNAs) and TiO_2 nanowires (TNWs) in UV photosensor

A considerable amount of literature has been studied on controlling the nanostructures of TiO_2 to enhance the responsivity of the UV photosensor. Granular-like and porous nanocrystalline TiO_2, for instance, provides a high reactive surface area to enhance the detection. However, the granular-like structure has deficiency on charge carrier's mobility in attribution to multiple grain boundaries, which hinder the transportation of charge carriers. Recently, researchers have shown an increased interest in one-dimensional (1-D) nanostructure of TiO_2 nanorod arrays (TNAs) and TiO_2 nanowires (TNWs) for UV photosensor applications due to their unique and excellent characteristics on size and shape, as well as their optical, electrical, and physical and chemical properties. Structures of TNAs and TNWs show high aspect ratio (length/diameter) larger than 1, with outstanding charge carrier's mobilities that are extremely suitable for a UV-sensing device. The size and shape may influence the optical property and give different performance on the photosensing device. Therefore, control over the shape and size depending on the method and experimental parameters used to synthesize the nanorods' structure has been one of the vital and challenging tasks. TNAs or TNWs offer a direct carrier's pathway, which increased the transportation rate and enhanced the performance of photosensor, as well as a photovoltaic type of optoelectronic devices [16, 17].

Previous research has established that the single-crystal 1D TNAs or TNWs could be synthesized via physical vapor deposition (PVD) method [18, 19] and chemical vapor deposition (CVD) [20]. Others are such as sol-gel coating, anodic oxidation, metal-organic chemical vapor deposition (MOCVD), template-assisted and sol-gel hydrothermal-based technique. Conversely, the synthesization and the deposition on the substrate for most techniques have required advanced instrumentation, for example of having a high pressured chamber, high temperature condition, or both, and addition of multiple procedures. Among those techniques, a one-step sol-gel hydrothermal method is preferred and widely investigated for their facile, rapid and considerably low temperature of synthesization and deposition technique.

Cao et al. deposited highly oriented TNAs on an FTO-coated glass substrate (**Figure 2**) and implemented amperometric measurement in 0.5-M sodium sulfate aqueous solution to investigate the photogenerated current responses under UV radiation [17]. TNAs were synthesized via a hydrothermal technique in a Teflon-lined stainless-steel autoclave, with sol-gel containing 10 mL of deionized (DI) water, 10 mL of HCl, and 0.4–0.8 mL of titanium butoxide for 4–24 hours at 120–180°C. The result presented in this study suggested that the TNAs with 40–60 nm in diameter and 6.0 μm in length were deposited for 4 hours at 150°C. The TNAs however aggregated at the bottom and only detached at tips. The TNAs were also congregated at higher temperature (180°C), with size increased to 50–100 nm in diameter and 2.0 μm in length, and in contrast, decrease to 20–40 nm in diameter and 0.5 μm in length at lower temperature (120°C). The titanium precursor (titanium butoxide) was also influenced the growth of the TNAs, as the size increased in correlation with the concentrations. However, the alignment of the nanorods was reduced at low concentration than that of higher concentration. The diameter size of the TNAs was also increase in correlation with time, even though the growth in length was hindered due to collision among the nanorods and aggregated to bigger size of nanorods. The dark current was found to be negligible without any radiation and the measured photogenerated current of 47.69 $\mu A/cm^2$ was achieved under the radiation (100 mW/cm^2), and linearly dependent on radiation intensity. Sample with higher specific surface area with separated nanorods showed better performance, and the designed UV photosensor corresponded well to 365 nm light. They also suggested that the small dimension and rod-shaped TNAs was important parameters for better mobility of charge carriers and light harvesting.

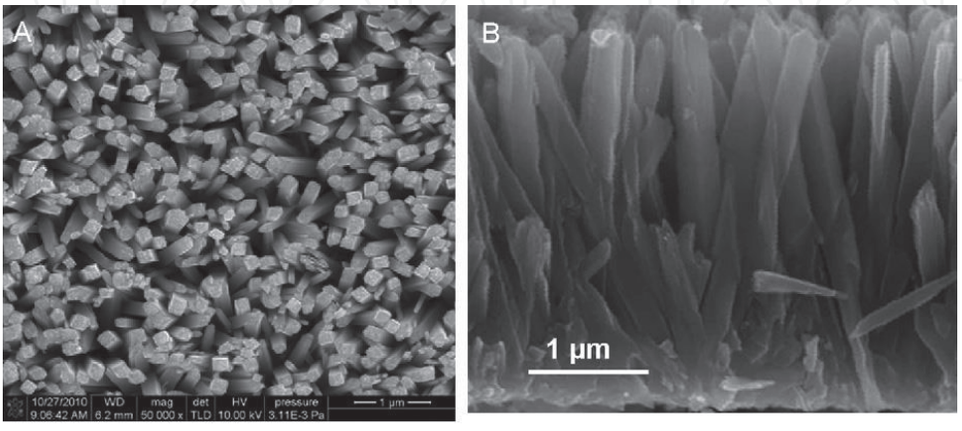

Figure 2. FESEM images of (A) top-view, and (B) cross-section of deposited TNAs film on FTO substrate at 150°C for 4 hours [17].

http://dx.doi.org/10.5772/intechopen.68460

One study by Xie et al. examined the growth of TNAs on an FTO-coated glass substrate via a hydrothermal technique at low temperature (180°C, 2 hours) for the application of UV photosensor, using water electrolyte [2]. TNAs were synthesized via a hydrothermal technique in a Teflon-lined stainless-steel autoclave, with sol-gel containing deionized (DI) water, HCl, and titanium tetrachloride. A pure single-crystalline rutile phase of tetragonal-shaped TNAs was consistently deposited on the substrate with 100–150 nm in diameter. A high photogenerated current of 4.67 μA and open circuit voltage of 0.408 V were achieved under the UV radiation (365 nm, 61.9 μW/cm^2) at 0 V bias and linearly dependent on radiation intensity. The maximum responsivity of 0.025 A/W was achieved at 310-nm wavelength. The fabricated device also showed a fast response time of 0.15 s (rise) and 0.05 s (decay). In contrast to the proposed device structure, they initiated that the photoconductivity-based mechanism possessed much longer recovery time in behalf of the existence of depletion region at the surface of the material, which created electrons trap. It has been suggested that the formation of built-in Schottky barrier at TNAs/water interface separated the photogenerated charge carriers under the UV radiation without application of external bias and produced photogenerated current. Thus, the fabricated device works on both photodiode and photovoltaic modes.

Xie et al. also studied the growth of TNAs on an FTO-coated glass substrate via a hydrothermal technique with similar sol-gel at low temperature (180°C, 2 hours) for a PEC-based UV photosensor, using a liquid crystal-embedded electrolyte [21]. It has been shown that gap between TNAs was filled by the electrolyte, which contributed to the increase of charge separation and transportation. The purpose of having the TNAs to create quasi-solid-state electrolyte was to increase the pathway of the optical light within the PEC structure through the light-trapping mechanism, which suggested to enhance the light absorption efficiency and thus increased the photogenerated charge carriers. An increased photogenerated current of 175 μA/cm^2 and open circuit voltage of 0.46 V were achieved under the UV radiation (365 nm, 2.5 mW/cm^2) at 0 V bias and linearly dependent on radiation intensity. The maximum responsivity of 0.09 A/W was achieved at 383-nm wavelength. The fabricated device also showed fast response time (less than 0.03 s) for both rise and decay times.

Yanru et al. fabricated a PEC-based UV photosensor with nanobranched TiO_2 arrays on an FTO-coated glass substrate as a photoanode and deposited via a two-step chemical synthesis process [22]. TNAs were synthesized via a hydrothermal technique in a Teflon-lined stainless-steel autoclave, with sol-gel containing deionized (DI) water, HCl, and titanium tetrachloride for 2 hours at 180°C. Nanobranches were synthesized via aqueous chemical growth on the TNAs through immersion in titanium tetrachloride solution for several hours at 25°C. The nanobranched TNAs showed lower transmittance than that of the bare TNAs due to increase of light absorption, which attributed to increase of light scattering within the nanostructures. The photogenerated current of 31 μA/cm^2 and open circuit voltage of 0.32 V were achieved for bare TNAs, while photogenerated current of 373 μA/cm^2 and open circuit voltage of 0.44 V were achieved for TNAs with 18-hour deposition of nanobranches both under the UV radiation (365 nm, 2 mW/cm^2) at 0 V bias. The peak responsivity was increased linearly with the increased of the nanobranches. It has been described that the improved responsivity was due to increase of light scattering and contacting surface area between TNAs with nanobranches and the electrolyte. In addition, ultrathin nanobranches reduced the recombination of electron-hole pair through a very efficient hole transportation to the TiO_2/electrolyte interface.

However, further increased in length of the nanobranches disconnected the branches from the TNAs and thus reduced the active surface area interconnection with the electrolyte.

A hybrid UV photosensor using the TNWs and poly (9,9-dihexylfluorene) (PFH) was reported by Zhang et al. on an FTO-coated glass substrate [23]. TNWs were synthesized via a hydrothermal technique in a Teflon-lined stainless-steel autoclave, with sol-gel containing toluene, tetrabutyltitanate, titanium tetrachloride, and HCl for 12 hours at 150°C. PFH was spin coated onto the deposited TNWs, and 1 mm^2 of Au electrode deposited on top of the hybrids. It has been shown that the TNWs (22.6 nm diameter size) were uniformly deposited on the substrate with constant density and size distribution. The PFH was filled and concealed the whole TNWs to avoid a direct contact between the TNWs and Au electrode and thus effectively formed the TNWs/PFH heterojunction. The absorption region was formed at 320–390 nm through the spectrum overlapping of TNWs/PFH hybrid film. The *I–V* characteristics showed a typical rectifying behavior through the formation of the TNWs/PFH heterojunction, with low dark current (0.19 μA/cm^2) at 2 V reverse bias. The photogenerated current of 0.75 μA and maximum responsivity of 568 mA/W were achieved under the UV radiation (330 nm, 132 μW/cm^2) at 2 V reverse bias and linearly dependent on the voltage bias. The photogenerated carriers were instantly collected by both electrodes under the irradiation of UV owing to the direct pathway of the TNWs and rapid charge carrier's separation at the heterojunction. It has been demonstrated that the improved responsivity could be achieved through the energy level matching between the TiO_2 and PFH, which smoothed the charge transportation at the interface and reduced the recombination between electrons and holes. The energy level matching assisted the transportation of holes from the valance band of TiO_2 to the highest occupied molecular orbit (HOMO) of PFH and electrons from the lowest unoccupied molecular orbital (LUMO) of PFH to the conduction band of TiO_2.

Another hybrid structure of TNWs/polyaniline nanoflowers (TNWs/PANI NFs) on an FTO-coated glass substrate was used to fabricate a multilayer device of FTO/TNWs/PANI NFs/TNWs/FTO (**Figure 3**) by Zu et al. for the application of self-power UV photosensor [15]. TNWs were synthesized via a hydrothermal technique in a Teflon-lined stainless-steel autoclave, with sol-gel containing deionized (DI) water, HCl, and titanium butoxide for 20 hours at 150°C. PANI NFs were deposited on the TNWs by *in situ* wet chemical deposition method at about 0–5°C for 1 hour per layer, before functionalized by the immersion method in PSS solution for 12 hours. It has been shown that the tetragonal shape of TNWs (~140 nm diameter, ~2 μm length) were uniformly deposited on the substrate with very high density and high-aspect ratio. The nonlinear and asymmetric *I–V* characteristics showed a typical rectifying behavior through the formation of a p-n heterojunction of p-type PANI NFs and n-type TNWs. In addition, the used of PSS further enhanced the photogenerated current of the UV photosensor. The photogenerated current of 0.8 μA (1 layer), 2.7 μA (23 layer), and 8.0 μA (5 layer) was achieved under the UV radiation (365-nm wavelength) at 0 V bias and linearly dependent on the thickness of deposited PANI NFs. It has been described that the inner potential difference was formed at the interface of TNWs/PANI NFs under the UV irradiation, which contributed to the separation of the photogenerated electron-hole pairs and thus forming the photocurrent.

http://dx.doi.org/10.5772/intechopen.68460

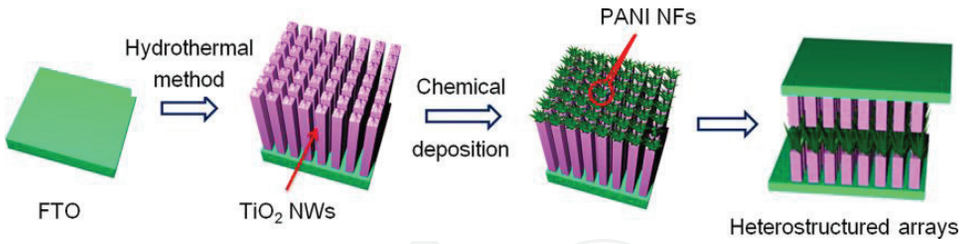

Figure 3. Schematic of the fabrication of TNWs/PANI NFs/TNWs heterostructured UV photosensor [15].

Yan et al. introduced an enhanced responsivity of self-powered UV photosensor using electrochemically reduced TNAs (R-TNAs) on an FTO-coated glass substrate [24]. TNAs were synthesized via a hydrothermal technique in a Teflon-lined stainless-steel autoclave, with sol-gel containing HCl aqueous solution and tetrabutyltitanate for 2 hours at 180°C. It has been shown that the TNAs (~100–150 nm diameter, ~3–3.5 μm length) were deposited nearly perpendicular to the substrate. The R-TNAs were prepared under –1.8 V (vs. SCE) in a conventional three-electrode system, and a disordered shell (~4 nm) with inconsistent distances between the adjacent lattice planes was formed at the outer layer of the TNAs. The disordered shell was suggested to be in correlation with bias voltage and reaction time and attributed to the electrochemical reduction. The photogenerated current of 0.24 mA/cm^2 was achieved for bare TNAs, while photogenerated current of 0.39 mA/cm^2 was achieved for R-TNAs, both under the UV radiation (385 nm, 4 mW/cm^2) at 0 V bias. The responsivity was increased linearly with the increased of the illumination intensity. High responsivity of 0.09 A/W was achieved under the UV intensity (385 nm, 1.6 mW/cm^2). The fabricated device also showed fast response time (less than 3 ms) for both rise and decay times than that of bare TNAs (4 ms) due to increase of charge transfer in the disordered shell. In addition, the open circuit voltage of the R-TNAs was higher than that of bare TNAs, which attributed to fast accumulation of holes in the disordered shell and decrease recombination of photogenerated charged carriers in the TNAs.

In previous studies on TNAs or TNW-based UV photosensor, the application of rod-like or wire-like structure of TiO_2 material has a lot of advantages over granular-like nanostructure, comprising high mobility of charge carriers and low carriers trapping at the grain boundaries, which contributed to high photogenerated current, high responsivity, and fast response and recovery times. The considerably high surface-to-volume ratio of the nanostructure also leads to miniaturization of the device and somehow reduces the power consumption for the passive device. Thus far, a number of studies have highlighted the factors that are associated with the high responsivity of nanostructured devices in correlation with high surface-to-volume ratio, surface defects, light trapping, charge carriers trapping, and high porosity.

Much of the current literature on TNAs or TNW-based UV photosensor has paid particular attention on the PEC-based structure due to their low cost, facile fabrication process, high contact area to the electrolyte, low recombination of the excitonic charge carriers, high photocurrent gain, and fast response and recovery times. Yanru et al. indicated that the PEC-based photosensor effectively evaded the utilization of complex epitaxial processes and the use of high-cost single-crystal substrates, which has been highly required for optoelectronic applications [22].

The existing literature on TNAs or TNWs-based UV photosensor also indicated that PEC-based devices worked in "self-powered" mode, which did not require any additional voltage supply from batteries or external supplies in order to operate. Thus, the PEC-based UV photosensor could be prominently reduced the size, independency and mobility of the whole detection system, and partly fulfilled the challenges for large-scale area applications of the sensors.

4. TiO_2 nanorod arrays in an ultraviolet photosensor via a facile one-step immersion method

There are a number of studies reported on the attempted hydrothermal method to prolong the synthesization and deposition processes of a preferred TNA film in attribution to the technical prospective of the TNAs, which is estimated to be remarkably enhanced if a fine-tuning of nanorods morphology is somehow achieved in the application of UV photosensor. Although the method has been extensively investigated by a number of researchers to enhance the deposition process on the substrate, the use of high-pressure vessel or autoclave even under low temperature condition was commonly reported. The usage of the tools was also difficult in attribution to the size and weight of the stainless steel materials and the Teflon line inside to hold the heat and the pressure inside the container. The time taken to heat the autoclave during the deposition process and cooling after the deposition procedure will somehow affect the deposited sample and included in the whole deposition process. Therefore, it is essential to improve the current method to a more simple, rapid, and consistent one-step sol-gel immersion method to synthesized and deposit the TNAs on the substrate.

In our process, we have synthesized and deposited the TNAs using an enhanced one-step sol-gel immersion method via a simple-modified Schott bottle with cap clamps as described in our former report [25]. The use of Schott bottle (**Figure 4**) as a glass container in our studies was intentionally to replace the use of stainless steel–based autoclave for the deposition of thin film TNAs at low temperature. The utilization of glass container was also to further

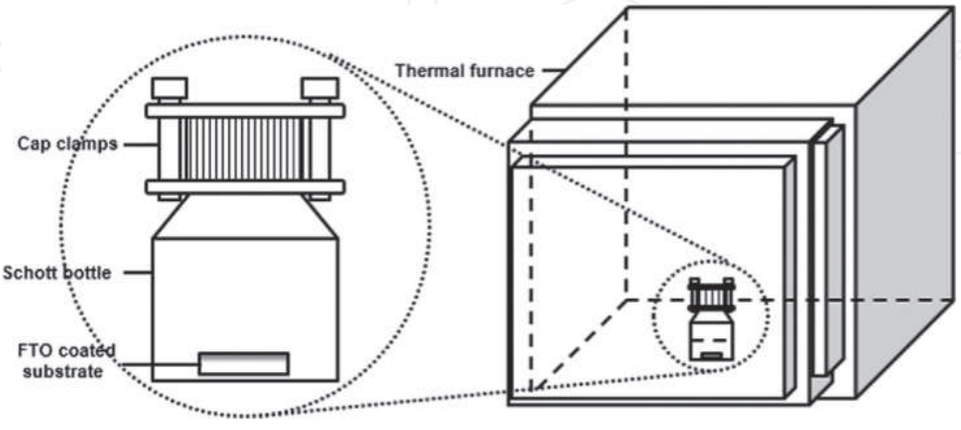

Figure 4. Setup for TNAs synthesis in a Schott bottle with cap clamps [25].

http://dx.doi.org/10.5772/intechopen.68460

enhance the investigation on the deposition of the thin film TNAs at low temperature and low time growth parameters for the purpose of optimization, simplification, and miniaturization of the device. In addition, the condition of sol-gel solution in the glass container also could be monitored and controlled manually, or by implementation of automation system to maintain the quality of the deposited film, which is highly essential in product manufacturing, especially during mass production.

In general, most of the sol-gel methods for synthesizing nanomaterials involve precursor, solvent, and stabilizer. The precursor provides the core composition of atoms or ions of the intended nanostructures, while the stabilizer component is added to control the growth rate of the nanoparticles in the solution, or epitaxially growth on the surface substrate. The presence of stabilizer in sol-gel minimized the reaction rate from developing instant precipitation or large aggregation, to some extent at room temperature. In our method, TNAs were prepared by a sol-gel immersion method as described in our previous work [25]. The FTO-coated glass substrate was used as the catalyst for the growth of the TNAs. The substrate was initially cleaned with acetone, ethanol, and DI water for 10 minutes subsequently in an ultrasonic water bath (Hwasin Technology Powersonic 405, 40 kHz). Sol-gel containing HCl (37 %, Merck) and DI water in a 1:1 volume ratio was prepared in a Schott bottle. After constant stirring for 10 minutes, 0.07 M of titanium (IV) butoxide (97%, Sigma-Aldrich) was slowly added in the prepared solution and stirred vigorously for another 30 minutes. The cleaned substrate was immersed in the sol-gel inside the Schott bottle. Once the conductive side of the substrate was placed at the bottom and facing upward, the bottle was then tightly sealed with a cap and clamped to attain the internal pressure throughout the deposition process at 150°C in an oven. After the TNAs were deposited at the elevated temperature for 2 hours, the bottle was immediately cooled down until the sample could be taken out from the bottle. The sample was then rinsed with DI water and dried at room temperature. Finally, the sample was annealed in a furnace at 450°C for 30 minutes to improve crystallinity.

The surface morphologies and topography of the TNAs were observed via field-emission scanning electron microscopy (FE-SEM, ZEISS Supra 40VP) and atomic force microscopy (AFM, Park System), respectively. The crystallinity of the synthesized TNAs was characterized via X-ray diffraction (XRD, Shimadzu XRD-6000, Cu K-alpha radiation, wavelength 1.54 Å). The optical property was characterized using a UV-Vis-NIR spectrophotometer (Cary 5000). The synthesized and deposited TNA on FTO-coated glass substrate was used as an electrode in the proposed fabrication of UV photosensor based on PEC structure. PEC structure was selected for our intention to design a UV photosensor to operate at low-powered and self-powered modes as previously described. The counter electrode was designed using platinum (Pt)-coated FTO-coated glass substrate. Both electrodes were compiled together, with a spacer (Surlyn, DuPont) in between the electrodes, with effective area designed approximately at 1.0 cm^{-2} in the centre of the device. The prepared electrolyte comprising 0.5 M of sodium sulfate (Na_2SO_4) was filled in the inner side of the spacer between the two electrodes.

5. Performance of synthesized TNAs-based UV photosensor

The proposed sol-gel immersion method is used for the development of a one-dimensional growth of uniform and densely array of nanorods structure. TNAs (120 nm diameter, 1.52 μm in length) were successfully synthesized and deposited on the FTO-coated glass substrate, as shown in **Figure 5**. The topography images of AFM (**Figure 6**) exhibited the comparable image structure of the top view as observed using FESEM. The measured root mean square roughness, R_{rms}, and average roughness, R_a, of the synthesized TNAs were approximately 38.52 and 30.37 nm, respectively. In general, the growth of TNAs is basically formed via the chemical reactions throughout the nucleation and growing processes through the hydrolysis of titanium(IV) butoxide in acidic solution. The proposed reaction mechanisms were emphasized on two steps as follows [25, 26]:

$$\mathrm{Ti}\left(\mathrm{OCH_2CH_2CH_2CH_3}\right)_4 + 4\,\mathrm{H_2O} \xrightarrow{\mathrm{HCl}} \mathrm{Ti(OH)_4} + 4\mathrm{ROH}, \tag{1}$$

$$\mathrm{Ti}(OH)_4 \;\rightarrow\; \mathrm{TiO_2} + 2\,\mathrm{H_2O}, \tag{2}$$

where R = C_4H_9.

At a regular state, the process of hydrolysis for titanium yields a definite amount of heat and occurs immediately at room temperature. The HCl was used as a stabilizer in the sol-gel to minimize the reaction rate from instantly developing precipitation or aggregation during the preparation stage, in attribution to the presence of free H^+ [27, 28]. At the same time, the 1D growth of TNAs at the preferred [001] direction was due to the presence of Cl^-, which bonded to the (1 1 0) plane and preventing the growth of TiO_2 crystal structure at its direction, to some extent [16, 29].

The crystal clear condition of the prepared sol-gel at room temperature showed the sufficiency of HCl content in the solution. Eq. (1) exhibits the hydrolysis process of titanium, which removes four carbon atoms from the precursor to form titanium hydroxyl and alkoxy group. The presence of H^+ through the addition of HCl as the stabilizer in this equation prevents the hydrolysis rate of titanium. The condensation process in Eq. (2) synthesizes TiO_2 and produces water. In order to produce highly aligned 1D growth of the TNAs from titanium alkoxide in the sol-gel, the ratio of DI water and HCl, and the growth rate through time and temperature need to be tuned and optimized. On heating during the sol-gel immersion process, the growth rate increases in correlation with synthesization and deposition time, which contributes to the

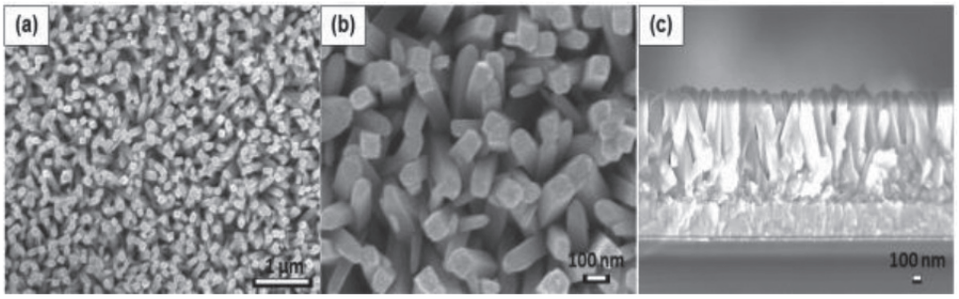

Figure 5. FESEM images of the TNAs at magnifications of (a) 20,000× and (b) 70,000×. (c) Cross-sectional images of the synthesized TNAs.

http://dx.doi.org/10.5772/intechopen.68460

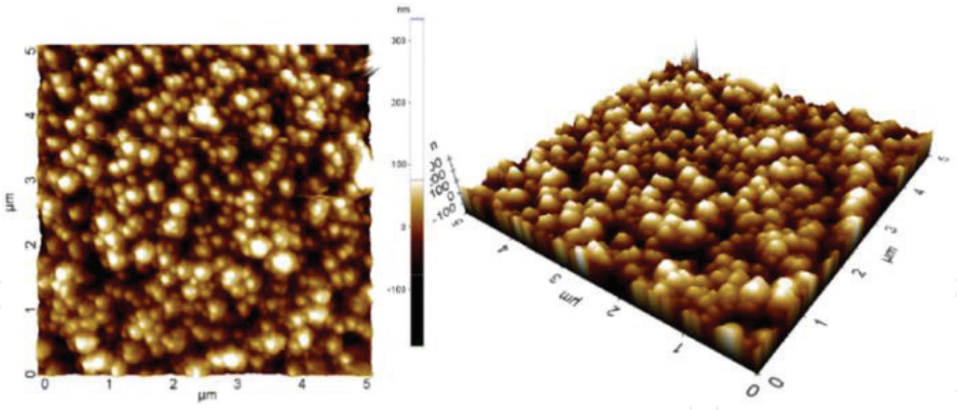

Figure 6. AFM images of the synthesized TNAs [25].

nucleation of TiO_2 on the seeds of FTO from the substrate. The nucleation of TiO_2 is basically based on the atomic structuring of TiO_6 octahedron as the fundamental unit, which plays an important role in the formation of tetragonal structure of TiO_2. The arrangement and interconnection of TiO_6 octahedral determine the phase and structure of the synthesized TiO_2. The rutile phase of TNAs synthesized in our method indicated that the edge sharing of TiO_6 octahedral occurred during the formation of tetragonal structure of TiO_2.

Figure 7 shows the XRD pattern of the synthesized and deposited TNAs. The rutile peaks of TiO_2 were detected at (1 0 1), (2 1 0), (2 1 1), (3 1 0), (0 0 2), and (1 1 2) planes, and no peaks which indicated the anatase and brookite phases observed in the pattern (JCPDS No.01-072-1148). Intense peaks at (0 0 2) and (1 0 1) planes showed that the 1D growth of TNAs was at the [0 0 1] direction.

Figure 8(a) shows the spectrum of optical absorbance of the synthesized and deposited TNAs on the FTO-coated glass substrate in a range of 200–800 nm. The spectrum exhibits that the intensity of the absorbance is significantly increased below 400-nm wavelength, which is in the UV region. Therefore, the optical characteristic of the deposited TNAs to absorb the UV radiation could be utilized for the application of UV photosensor as predicted. The performance of the developed UV photosensor was measured under 365-nm UV radiation at a bias voltage of 1 V. **Figure 8(b)** exhibits the time-dependent photogenerated current of the developed UV photosensor using the deposited TNAs. The result shows an average increase of 0.1 mA of photogenerated current under UV radiation, which is attributed to the photogenerated electrons through the excitation from the valance band into the conduction band. The rise and fall times are negligible throughout the measurement. Thus, the fabricated UV photosensor from the deposited TNAs facilitates the potential application in a low-power UV detecting device.

The present study was designed to introduce a new one-step method to synthesize and deposit a thin film TNAs on the FTO-coated glass substrate at low temperature and rapid process using the facile glass container for the application of UV photosensor. Although the fabricated UV photosensor has successfully shown its potential application in sensing the UV radiation, more research is required to determine the optimum efficiency of the device, through the variation of synthesization and deposition parameters, composition of electrolytes, composition of sol-gel, device structure, and many more. This research has opened up many opportunities of further investigation.

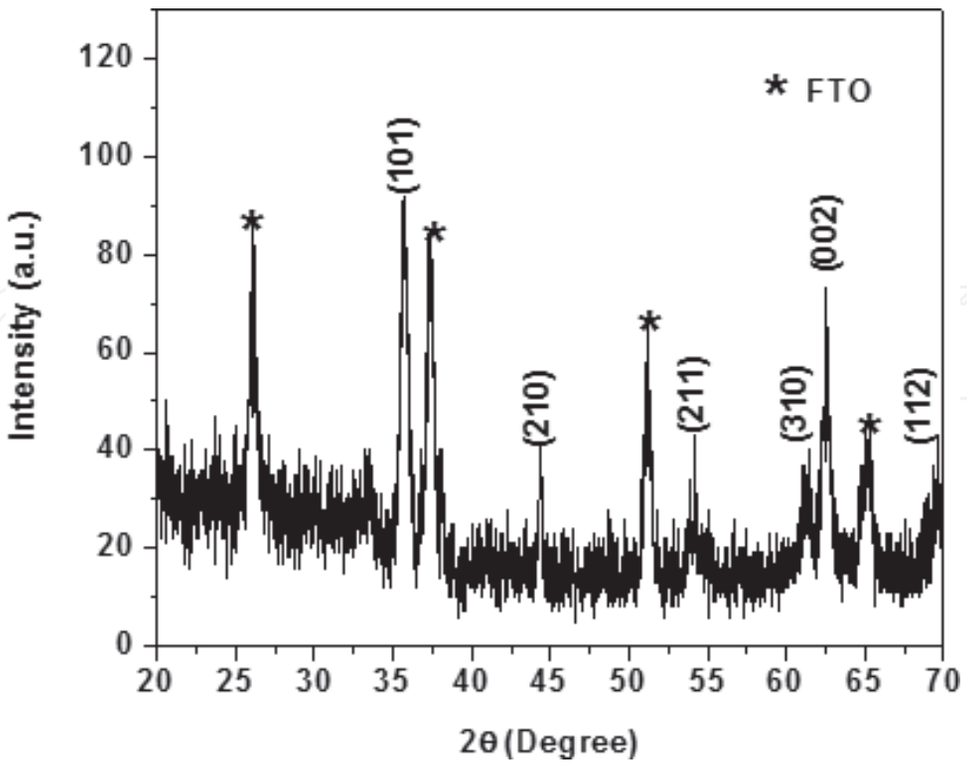

Figure 7. XRD pattern of the rutile-phased TNAs [25].

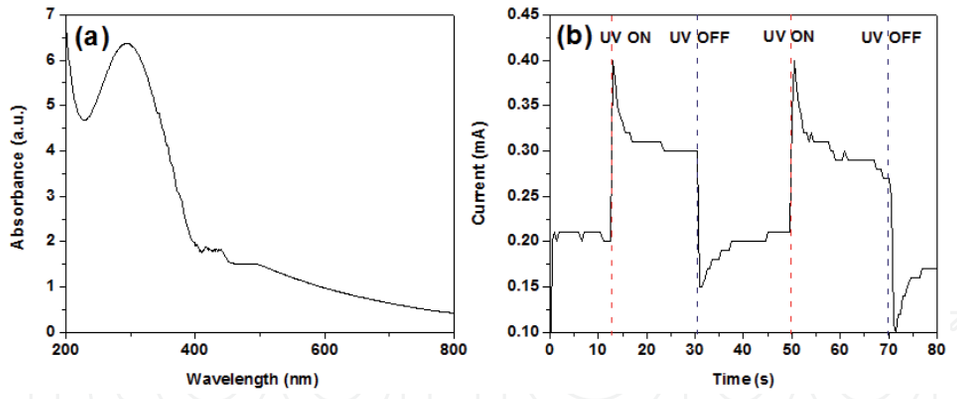

Figure 8. (a) UV-Vis absorbance spectrum, (b) photocurrent response under UV irradiation (365 nm, 1 V bias) of synthesized TNAs [25].

6. Conclusion

The aim of the present study was to examine the previous works on TiO_2 nanostructures in the application of UV photosensor and consequently open up new possibilities and opportunity in future works for enhancing the development of the device. This study has found that the nanostructured materials have a lot of advantages over bulk materials, and the high

responsivity of the UV photosensor was mostly associated with the high surface-to-volume ratio, porosity, surface defects, light trapping, intensity of the UV radiation, and low-charge-carriers trapping. One-dimensional growth of TNAs or TNWs offers an enhance charge carriers mobility to overcome the photocurrent loss due to the existence of multiple grain boundaries in granular-like and porous nanostructures with comparatively high surface-to-volume ratio. The performance of the device was also dependent on the device structure and the detection mechanism of photon through the photogenerated charge carriers. PEC-based device structure is preferred the TNA-based UV photosensors due to their low cost, facile fabrication process, high contact area to the electrolyte, low recombination of the excitonic charge carriers, high photocurrent gain, and fast response and recovery times. It also could work in an applied bias mode, as well as in 'self-powered' mode, which did not require any additional voltage supply. Besides the high responsivity, the design of the device also needs to fulfill the requirement for small size, independency and mobility of the whole detection system. Our study was designed to introduce a new one-step method to synthesize and deposit a thin film TNAs on an FTO-coated glass substrate at low temperature and rapid process using a facile glass container. The fabricated PEC-based UV photosensor using the deposited TNAs has successfully shown its potential application in sensing the UV radiation. Our introduced method has opened up many opportunities of further investigation in the development of 1D growth of TNAs for various device applications.

Acknowledgements

This work was financially supported by the Fundamental Research Grant Scheme 600-RMI/FRGS 5/3 (57/2015)) from the Ministry of Education Malaysia. The authors also would like to thank the Faculty of Electrical Engineering (FKE), NANO-ElecTronic Centre (NET), NANO-SciTech Centre (NST), Research Management Centre (RMC) of University Teknologi MARA, Shah Alam, Malaysia (UiTM), the Ministry of Higher Education of Malaysia, and International Islamic University Malaysia (IIUM).

Author details

Marmeezee Mohd. Yusoff[1,3], Mohamad Hafiz Mamat[1,2]* and Mohamad Rusop Mahmood[1,2]

*Address all correspondence to: hafiz_030@yahoo.com

1 Faculty of Electrical Engineering, NANO-ElecTronic Center (NET), University Teknology MARA (UiTM), Shah Alam, Selangor, Malaysia

2 NANO-SciTech Centre (NST), Institute of Science (IOS), University Teknology MARA (UiTM), Shah Alam, Selangor, Malaysia

3 Manufacturing and Materials Engineering Department (MME), Kulliyyah of Engineering, International Islamic University Malaysia (IIUM), Malaysia

References

[1] Pfeifer V, Erhart P, Li S, Rachut K, Morasch J, Brötz J, Reckers P, Mayer T, Rühle S, Zaban A, Mora Seró I, Bisquert J, Jaegermann W, Klein A. Energy band alignment between anatase and rutile TiO_2. The Journal of Physical Chemistry Letters. 5 December 2013;**4**:4182–4187

[2] Xie Y, Wei L, Wei G, Li Q, Wang D, Chen Y, Yan S, Liu G, Mei L, Jiao J. A self-powered UV photodetector based on TiO_2 nanorod arrays. Nanoscale Research Letters. 2013;**8**:188

[3] Cao G, Wang Y. Nanostructures and Nanomaterials: Synthesis, Properties, and Applications. 2nd ed. New Jersey: World Scientific; 2011

[4] Soci C, Zhang A, Bao XY, Kim H, Lo Y, Wang D. Nanowire photodetectors. Journal of Nanoscience and Nanotechnology. March 2010;**10**:1430–1449

[5] Okuya M, Shiozaki K, Horikawa N, Kosugi T, Kumara GRA, Madarász J, Kaneko S, Pokol G. Porous TiO_2 thin films prepared by spray pyrolysis deposition (SPD) technique and their application to UV sensors. Solid State Ionics. 2004;**172**:527–531

[6] Xue H, Kong X, Liu Z, Liu C, Zhou J, Chen W, Ruan S, Xu Q. TiO_2 based metal-semiconductor-metal ultraviolet photodetectors. Applied Physics Letters. 2007;**90**:201118

[7] Han Y, Wu G, Wang M, Chen H. High efficient UV-a photodetectors based on monodispersed ligand-capped TiO_2 nanocrystals and polyfluorene hybrids. Polymer. 2010;**51**:3736–3743

[8] Vigil E, Peter LM, Forcade F, Jennings JR, González B, Wang H, Curbelo L, Dunn H. An ultraviolet selective photodetector based on a nanocrystalline TiO_2 photoelectrochemical cell. Sensors and Actuators A: Physical.2011;**171**:87–92

[9] Li X, Gao C, Duan H, Lu B, Pan X, Xie E. Nanocrystalline TiO_2 film based photoelectrochemical cell as self-powered UV-photodetector. Nano Energy. 2012;**1**:640

[10] Xiang WF, Yang PR, Wang AJ, Zhao K, Ni H, Zhong SX. Vertical geometry ultraviolet photodetectors with high photosensitivity based on nanocrystalline TiO_2 films. Thin Solid Films. 2012;**520**:7144–7146

[11] Lv K, Zhang M, Liu C, Liu G, Li H, Wen S, Chen Y, Ruan S. TiO_2 ultraviolet detector based on $LaAlO_3$ substrate with low dark current. Journal of Alloys and Compounds. 2013;**580**:614–617

[12] Selman AM, Hassan Z, Husham M, Ahmed NM. A high-sensitivity, fast-response, rapid-recovery p–n heterojunction photodiode based on rutile TiO_2 nanorod array on p-Si(1 1 1). Applied Surface Science. 2014;**305**:445–452

[13] Liu G, Tao C, Zhang M, Gu X, Meng F, Zhang X, Chen Y, Ruan S. Effects of surface self-assembled NH_4^+ on the performance of TiO_2-based ultraviolet photodetectors. Journal of Alloys and Compounds. 2014;**601**:107

[14] Yang J, Jiang Y-L, Li L-J, Muhire E, Gao M-Z. High-performance photodetectors and enhanced photocatalysts of two-dimensional TiO_2 nanosheets under UV light excitation. Nanoscale. 2016;**8**:8170–8177

[15] Zu X, Wang H, Yi G, Zhang Z, Jiang X, Gong J, Luo H. Self-powered UV photodetector based on heterostructured TiO_2 nanowire arrays and polyaniline nanoflower arrays. Synthetic Metals. February 2015;**200**:58–65

[16] Liu B, Aydil ES. Growth of oriented single-crystalline rutile TiO_2nanorods on transparent conducting substrates for dye-sensitized solar cells. Journal of the American Chemical Society. 25 March 2009;**131**:3985–3990

[17] Cao C, Hu C, Wang X, Wang S, Tian Y, Zhang H. UV sensor based on TiO_2 nanorod arrays on FTO thin film. Sensors and Actuators B: Chemical. 2011;**156**:114–119

[18] Meng L, Chen H, Li C, dos Santos MP. Preparation and characterization of dye-sensitized TiO_2 nanorod solar cells. Thin Solid Films. 2015;**577**:103–108

[19] Binetti E, El Koura Z, Bazzanella N, Carotenuto G, Miotello A. Synthesis of mesoporous ITO/TiO_2 electrodes for optoelectronics. Materials Letters.2015;**139**:355–358

[20] Chen JB, Wang CW, Kang YM, Li DS, Zhu WD, Zhou F. Investigation of temperature-dependent field emission from single crystal TiO_2 nanorods. Applied Surface Science. 2012;**258**:8279–8282

[21] Xie Y, Wei L, Li Q, Chen Y, Liu H, Yan S, Jiao J, Liu G, Mei L. A high performance quasi-solid-state self-powered UV photodetector based on TiO_2 nanorod arrays. Nanoscale. 2014;**6**:9116–9121

[22] Yanru X, Lin W, Qinghao L, Yanxue C, Shishen Y, Jun J, Guolei L, Liangmo M. High-performance self-powered UV photodetectors based on TiO_2 nano-branched arrays. Nanotechnology. 2014;**25**:075202

[23] Zhang M, Li D, Zhou J, Chen W, Ruan S. Ultraviolet detector based on TiO_2 nanowire array–polymer hybrids with low dark current. Journal of Alloys and Compounds. 2015;**618**:233–235

[24] Yan P, Wu Y, Liu G, Li A, Han H, Feng Z, Shi J, Gan Y, Li C. Enhancing photoresponsivity of self-powered UV photodetectors based on electrochemically reduced TiO_2 nanorods. RSC Advances. 2015;**5**:95939–95942

[25] Yusoff MM, Mamat MH, Malek MF, Suriani AB, Mohamed A, Ahmad MK, Alrokayan SAH, Khan HA, Rusop M. Growth of titanium dioxide nanorod arrays through the aqueous chemical route under a novel and facile low-cost method. Materials Letters. 2016;**164**:294–298

[26] Cozzoli PD, Kornowski A, Weller H. Low-temperature synthesis of soluble and processable organic-capped anatase TiO_2 nanorods. Journal of the American Chemical Society. 2003;**125**:14539–14548

[27] Li Y, Liu J, Jia Z. Morphological control and photodegradation behavior of rutile TiO_2 prepared by a low-temperature process. Materials Letters.2006;**60:**1753–1757

[28] Iraj M, Nayeri FD, Asl-Soleimani E, Narimani K. Controlled growth of vertically aligned TiO_2 nanorod arrays using the improved hydrothermal method and their application to dye-sensitized solar cells. Journal of Alloys and Compounds. 2016;**659**:44–50

[29] Feng X, Shankar K, Varghese OK, Paulose M, Latempa TJ, Grimes CA. Vertically aligned single crystal TiO_2nanowire arrays grown directly on transparent conducing oxide coated glass: Synthesis details and applications. Nano Letters. 12 November 2008;**8**:3781–3786